
# Copper chaperone blocks amyloid formation via ternary complex

*Quarterly Reviews of Biophysics*

**cambridge.org/qrb**

# Copper chaperone blocks amyloid formation via ternary complex

Istvan Horvath, Tony Werner, Ranjeet Kumar and Pernilla Wittung-Stafshede

Department of Biology and Biological Engineering, Chalmers University of Technology, 412 96 Gothenburg, Sweden

## Report

**Cite this article:** Horvath I, Werner T, Kumar R, Wittung-Stafshede P (2018). Copper chaperone blocks amyloid formation via ternary complex. *Quarterly Reviews of Biophysics* **51**, e6, 1–5. https://doi.org/10.1017/S0033583518000045

Received: 16 December 2017
Revised: 16 March 2018
Accepted: 20 March 2018

**Key words:**
Alpha-synuclein; amyloids; Atox1; copper chaperone; metal transport; protein misfolding

**Author for correspondence**:
P. Wittung-Stafshede, E-mail: pernilla.wittung@chalmers.se

**Abstract**

Protein misfolding in cells is avoided by a network of protein chaperones that detect misfolded or partially folded species. When proteins escape these control systems, misfolding may result in protein aggregation and amyloid formation. We here show that aggregation of the amyloidogenic protein $\alpha$-synuclein ($\alpha$S), the key player in Parkinson's disease, is controlled by the copper transport protein Atox1 *in vitro*. Copper ions are not freely available in the cellular environment, but when provided by Atox1, the resulting copper-dependent ternary complex blocks $\alpha$S aggregation. Because the same inhibition was found for a truncated version of $\alpha$S, lacking the C-terminal part, it appears that Atox1 interacts with the N-terminal copper site in $\alpha$S. Metal-dependent chaperoning may be yet another manner in which cells control its proteome.

## Introduction

Systemic and tissue imbalances of metal levels are often found in neurodegenerative disorders such as Parkinson's disease (PD) (Fink, 2006), implying that metal ions may play roles in disease progression. A unifying molecular event in all neurodegenerative disorders is misfolding and aberrant self-assembly of proteins into amyloid fibers with a hallmark cross-$\beta$-sheet arrangement. Conformational changes resulting in aggregation of the neuronal protein $\alpha$-synuclein ($\alpha$S) into amyloid fibers is directly related to PD (Galvin *et al.* 1999; Winner *et al.* 2011). Many synthetic as well as naturally occurring molecules can modulate $\alpha$S amyloid formation *in vitro*, for example ring-fused two-pyridones (Horvath *et al.* 2012), other amyloidogenic proteins (i.e., cross-reactivity) (Horvath & Wittung-Stafshede, 2016), bacterial proteins (Chorell *et al.* 2015) and metal ions (Davies *et al.* 2016; Montes *et al.* 2014).

Copper (Cu) in both redox states (oxidized = Cu(II); reduced = Cu(I)) can bind to $\alpha$S (Camponeschi *et al.* 2013; De Ricco *et al.* 2015a) and structural features, binding sites, and affinities for the interaction between $\alpha$S and Cu(II), as well as Cu(I), have been the focus of *in vitro* spectroscopic investigations (Binolfi *et al.* 2006, 2011; Camponeschi *et al.* 2013; De Ricco *et al.* 2015a), Fig. 1*a*. Although most divalent cations can accelerate $\alpha$S amyloid formation, Cu(II) has the largest such effect *in vitro* (Davies *et al.* 2016; Montes *et al.* 2014). Notably, the effect of Cu(I) binding on $\alpha$S amyloid formation *in vitro* has not been reported. It was recently suggested that $\alpha$S was able to act as a ferri-reductase, reducing iron using Cu(I)/Cu(II) as a catalytic redox center (Brown, 2013) but it awaits to be revealed if Cu-mediated redox reactions are related to $\alpha$S function or merely part of a cascade of deleterious processes (De Ricco *et al.* 2015b). It remains unknown how, and in what redox state, Cu would reach $\alpha$S *in vivo*. The cytoplasm is a reducing environment so most Cu ions are in the Cu(I) form (Hatori and Lutsenko, 2013); in addition, there is no free Cu in cells (Ohrvik & Thiele, 2014; Tottey *et al.* 2005; Waldron *et al.* 2009).

In cells, Cu(I) is transported by copper transport proteins to specific targets that require Cu for function (De Feo *et al.* 2009). Such an elaborate system is necessary for tight control of metal distribution in time and space, and in order to keep Cu(I) soluble as free Cu(I) is chemically instable. In the human cytoplasm, the Cu chaperone Atox1 (Fig. 1*b*), a small single-domain protein with a CXXC (C, cysteine; X, any residue) Cu-binding motif (Boal & Rosenzweig, 2009), brings Cu from the Cu importer Ctr1 in the plasma membrane to two large, multi-domain $P_{1B}$ type ATPases in the Golgi membrane, ATP7A and ATP7B, for loading of Cu-dependent enzymes (Lutsenko*et al.* 2007). Movement of Cu(I) between these transport proteins is facilitated by direct metal-bridged protein–protein complexes (Niemiec *et al.* 2015). Recently, new functions and partner proteins for Atox1 have been reported, implying an extended functional repertoire (Blockhuys & Wittung-Stafshede, 2017; Blockhuys *et al.* 2017).

If alterations in Cu levels are a cause or a consequence in amyloidogenic diseases is unclear. Perhaps Cu transport proteins deliver Cu(I) to $\alpha$S such that, possibly requiring Cu(I) to Cu(II) oxidation, aggregation is modulated? Or Cu transport proteins may instead be protective and



CAMBRIDGE UNIVERSITY PRESS

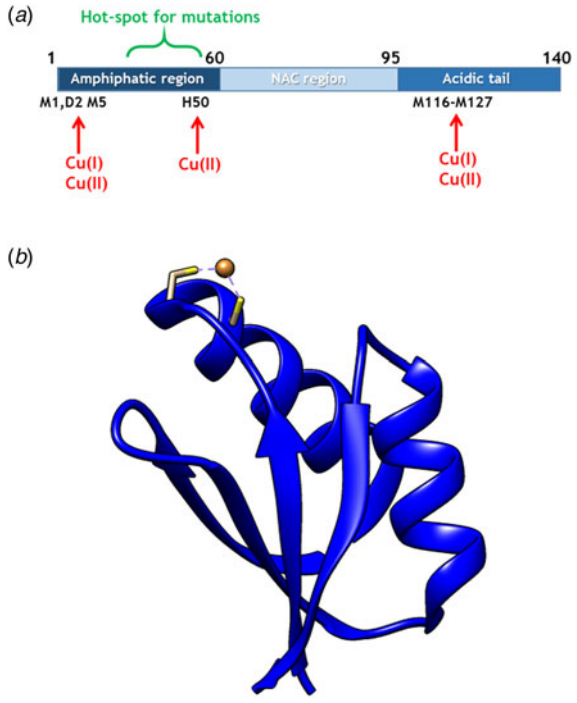


**Fig. 1.** (*a*) Scheme of $\alpha$S sequence (key parts noted) with Cu-binding sites indicated. (*b*) Structure of Atox1 with Cu ion and Cu-coordinating Cys highlighted (1TL4).

remove Cu from $\alpha$S before aggregation is triggered? We note that Atox1 and other Cu transporters are expressed in most neuronal cells (Davies *et al.* 2013; Montes *et al.* 2014); thus, interactions with $\alpha$S are feasible. To begin to address this knowledge gap, we here tested if Atox1 can deliver Cu(I) to $\alpha$S, and if so, what are consequences on amyloid formation.

## Materials and methods

### Proteins

A construct with the wild-type $\alpha$S gene was transformed into BL21(DE3) (Novagen) cells. Cells were first grown to $OD_{600}$ of 0.6 in LB containing 100 μg $ml^{-1}$ carbenicillin at 37 °C and then induced with 1 mM IPTG (isopropyl b-D-1-thiogalactopyranoside) and grown overnight at 25 °C. The cells were lysed by sonication in an ice bath through a sonicator probe in pulse mode (20 mM Tris–HCl buffer, pH 8.0) in the presence of a protease inhibitor cocktail (Roche). After sonication, the lysate was treated with a universal nuclease (Pierce) for 15 min at room temperature. The lysate was then heated at 90 °C for 10 min followed by centrifugation for 30 min at 15 000 g. After filtration through a 0.2 μm filter, the sample was loaded on to pre-equilibrated 5 mL HiTrap Q FF anion exchange column (GE Healthcare) and eluted by a linear gradient of 1 M NaCl in 20 mM Tris–HCl buffer pH 8.0. Fractions containing $\alpha$S were combined and concentrated with Ultra-15 Ultracel 10 K centrifugal filter devices (Millipore). The concentrate was loaded on to Hiload 16/600 Superdex 75 pg column (GE Healthcare) and retrieved in 20 mM Tris–sulfate buffer pH 7.4.

A pET3a construct (including a tag with a repressor protein and a His-stretch followed by a Caspase 7 cleavage site) of the variant $\alpha$S A107C was transformed into BL21(DE3) (Novagen) cells, which were then grown in similar conditions as for wild-type $\alpha$S. The cells were harvested by centrifugation and re-suspended in Buffer A (20 mM Tris–HCl pH 8, 20 mM imidazole and 8 M urea), then sonicated and centrifuged for 30 min at 15 000 g. The supernatant was filtered through a 0.2 μm filter and applied to pre-equilibrated 5 ml Hi Trap Ni-NTA column (GE healthcare) with buffer A. After washing the column with 5 column volumes of buffer B (20 mM Tris–sulfate pH 7.4, 20 mM imidazole, 50 mM NaCl), the protein was eluted with buffer B with 250 mM imidazole. The tag was cleaved by adding Caspase 7 in the ratio of 1:100 (caspase 7: $\alpha$S A107C w/w) in the presence of 5 mM TCEP (tris (2-carboxyethyl) phosphine) and incubated overnight at 4 °C. The cleaved protein was loaded onto a 5 mL HiTrap Q FF anion exchange column (GE Healthcare) and eluted by a linear gradient of 1 M NaCl in 20 mM Tris-sulfate buffer, pH 7.4. The eluted fractions were pooled, concentrated and loaded onto a Hiload 16/600 Superdex 75 column (GE Healthcare). The purified protein was eluted in 20 mM Tris–HCl buffer pH 7.4 with 1 mM TCEP. Truncated $\alpha$S (containing residues 1–97) was expressed using the same vector (pET3a) as the A107C $\alpha$S mutant and the purification followed the same procedure. The final gel filtration step was performed in 20 mM Tris–HCl buffer pH 7.4. Purified CCS was obtained from the Umeå University Protein Expertise Platform (http://www.kbc.umu.se/english/pep/services/).

Until use, $\alpha$S protein samples were frozen in liquid nitrogen and stored at −80 °C. Purity for $\alpha$S variants was confirmed by single bands on SDS–PAGE and single elution peaks in SEC. The concentrations of wild-type and A107C $\alpha$S were determined using $\varepsilon_{280} = 5960\ M^{-1}\ cm^{-1}$ (four Tyr; no Trp); $\varepsilon_{280} = 1490\ M^{-1}\ cm^{-1}$ was used for the truncated $\alpha$S (one Tyr).

Atox1 in a pET21(b) vector was transformed into BL21(DE3) plysS (Novagen) cells. Transformants were first grown to $OD_{600}$ of 0.6 at 37 °C, and then induced with 1 mM IPTG and grown for overnight at 25 °C. The cells were harvested by centrifugation and re-suspended in Buffer A (20 mM MES, 1 mM EDTA, 1 mM TCEP, pH 5.7) containing protease inhibitor cocktail (Roche), followed by sonication. The lysate was treated with a universal nuclease (Pierce) for 30 min at 4 °C and then centrifuged for 30 min at 15 000 g. After filtration through a 0.2 μm filter, the supernatant was loaded onto a pre-equilibrated 5 mL HiTrap SP HP cation exchange column (GE Healthcare). The protein was eluted by a linear gradient of buffer B (20 mM MES, 1 mM TCEP, 1 M NaCl, pH 5.7). Fractions containing protein of the correct molecular weight were pooled and concentrated with Ultra-15 Ultracel 3 K centrifugal filter devices (Millipore). The concentrated protein sample was loaded on to Hiload 16/600 Superdex 75 pg column (GE Healthcare) and retrieved in Chelex-treated storage buffer C (20 mM Tris-sulfate pH 7.4, 150 mM NaCl, 1 mM TCEP). The concentration of Atox1 was determined using $\varepsilon_{280} = 2980\ M^{-1}\ cm^{-1}$. Upon purification, Atox1 is eluted in the apo-form. Cu(I)-loading of Atox1 is achieved by the addition of equimolar Cu(II) in the presence of 5-fold excess 1,4-dithiothreitol (DTT), as previously reported (Niemiec *et al.* 2012, 2015).

### Amyloid formation assay

$\alpha$S amyloid formation reactions were conducted in 96-well half-area transparent bottom plates with a non-binding (non-ionic hydrophilic) surface (Corning, CLS3881) with one 2-mm glass bead in each well using a plate reader-incubator instrument (BMG Labtech, Fluostar Optima). Time-resolved measurements

were performed in TBS (0.05 M Tris–HCl buffer, pH 7.4 with 0.15 M NaCl; 93 318 Sigma-Aldrich) buffer in the presence of 20 μM Thioflavin T (ThT; T3516 Sigma-Aldrich) at 37 °C using 200 rpm agitation for 5 min during the 20 min measurement cycles. Samples were typically incubated for 60 h and fluorescence measured every 20 min. ThT was excited at 440 nm and emission was recorded at 480 nm. All ThT experiments were performed in triplicate at each time and repeated at least three independent times.

### Atomic force microscopy (AFM)

Aggregated samples from ThT experiments were diluted into MilliQ water (10–20 times) and deposited on freshly cleaved mica. After 10 min, the mica was rinsed with filtered Milli-Q water and dried under a gentle nitrogen stream. Images were recorded on an NTEGRA Prima setup (NT-MDT) using a gold-coated single crystal silicon cantilever (NT-MDT, NSG01, spring constant of ~5.1 N/m) and a resonance frequency of ~180 kHz. 512-pixel images were acquired with 0.5 Hz scan rate. Images were analyzed using the WSxM 5.0 software(Horcas *et al.* 2007).

### Size exclusion chromatography (SEC)

500 μl of samples containing 70 μM αS and/or 70 μM apo- or holo-Atox1 were injected on a Superdex 75 10/300 column (GE Healthcare) using an Äkta purifier (GE healthcare) system. Running buffer was 20 mM TRIS pH 7.6 with 150 mM NaCl and 350 μM DTT. Pre-mixing of Cu(II), DTT and apo-Atox1, results in Cu(I) loading of the protein, i.e., Cu-Atox1 (Niemiec *et al.* 2012, 2015). Elution profiles were probed by absorbance at two wavelengths in parallel: 280 nm (protein) and 254 nm (sulfur-to-Cu charge transfer). 1 ml fractions were collected and sent for metal analysis by ICP-MS (Chalmers ICP-MS facility). SEC was also used to quantify the amount of soluble αS after aggregation reactions. For such analysis, the aggregated samples were spun down (12 000 g, 15 min) and the supernatant loaded on the Superdex 75 10/300 column using the same conditions as for the fresh protein mixtures. The amount of αS was determined by peak intensity at 280 nm at the 9.5 ml elution volume corresponding to αS. The samples were also analyzed for protein content by SDS–PAGE electrophoresis.

### Surface plasmon resonance (Biacore)

The αS Ala107Cys variant was biotinylated with Ez-Link BMCC-Biotin (Cat. No.: 21900, Thermo Fisher Scientific) following the manufacturer's instructions. After the reaction, the mixture was loaded on an Enrich70 24 ml SEC (BioRad) using an NGC chromatography system (BioRad) to remove excess biotin. Biotinylated αS was immobilized on one channel of a streptavidin-coated sensor chip SA (GE Healthcare) to a level of ~1000 response units. Samples were injected for 180 s pulses in 10 mM HEPES pH 7.4 buffer containing 150 mM NaCl. Measurements were performed on a Biacore X100 instrument. The measured response units were background corrected by subtracting signal of the non-modified flow channel.

## Results and discussion

Purified αS aggregates into amyloid fibers *in vitro* upon incubation at pH 7, 37 °C and, with agitation, αS (70 μM) aggregates with a lag time of about 10–15 h, as determined using the ThT assay (Fig. 2*a*). Addition of 1:1 molar ratio of Cu(II) speeds up

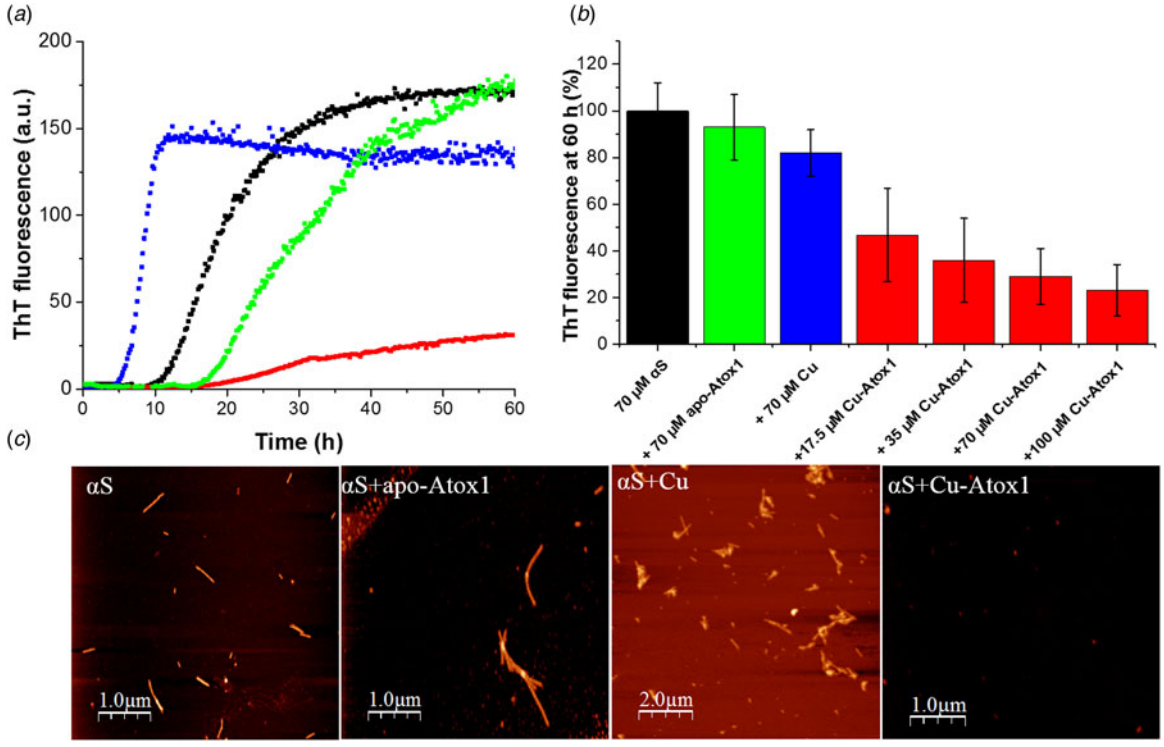


**Fig. 2.** (*a*) Representative ThT fluorescence curves probing amyloid formation of 70 μM αS alone (black), and in the presence of equimolar Cu(II) (blue), apo-Atox1 (green) and Cu-Atox1 (red). (*b*) Analysis of ThT emission at 60 h for different αS/Atox1 mixtures. Average values and standard deviations were calculated based on at least four repetitions. (*c*) AFM images of aggregation end-products in A.

aggregation (Fig. 2*a*), as expected. The presence of apo-Atox1 has only a small delaying effect on the lag time for aggregation, whereas Cu(I)-loaded Atox1 distinctly reduced αS amyloid formation in a concentration-dependent manner (Fig. 2*a,b*). Atomic force microscopy (AFM) revealed the presence of typical αS amyloids for samples with only αS, αS in the presence of Cu (II), and αS with apo-Atox1. In contrast, but in accord with the ThT data, in the presence of Cu(I)-Atox1, no αS amyloids were detected by AFM (Fig. 2*c*). Notably, aggregation experiments in the presence of Cu(I) (without Atox1, e.g. as a Cu(I)-DTT complex) are technically challenging, as Cu(I) will oxidize and/or precipitate during these typically 1–2 days long experiments. Instead, we used silver ions (Ag(I)) as a redox-inert model for Cu(I) ions that is stable in solution. Because the presence of equimolar $AgNO_3$ did not affect αS amyloid formation (Fig. S1A), it appears that the inhibitory effect of Cu-Atox1 arises due to the ternary complex formation, and not Cu(I) delivery to αS.

As a complement to the AFM (lack of observable amyloids) and ThT emission (low emission implying no amyloids) data for αS mixed with Cu-Atox1, quantification of soluble αS after aggregation experiments showed that there was much more monomeric αS when it was incubated with Cu-Atox1 as compared with when incubated alone or with apo-Atox1 (Fig. S2A). As a test of specificity, we probed the effect of another cytoplasmic Cu-chaperone, the copper chaperone for superoxide dismutase (CCS), on αS amyloid formation. However, the presence of Cu-loaded CCS had no effect on αS amyloid formation (Fig. S2B), implying that the Cu(I)-Atox1-mediated inhibition of αS aggregation is protein specific.

To test for direct interaction of Cu-Atox1 with αS, we turned to surface plasmon resonance (Biacore). Using αS attached to the surface of a Biacore chip via cysteine-modification, Atox1 binding was detected as an increase in the response signal which corresponds to the mass of bound material. Whereas apo-Atox1 did not interact with αS, we found a concentration-dependent interaction between αS and Cu(I)-Atox1 in the Biacore experiments. By fitting concentration-dependent endpoint response values, a dissociation constant for the Cu-Atox1/αS complex of around 5 μM was determined (Fig. 3*a*, Fig. S1B).

To probe the protein–protein pair further, we analyzed Cu-Atox1/αS mixtures with SEC. Initial mixtures contained concentrations of proteins similar to in the ThT aggregation experiments, which are then diluted during chromatography. SEC traces probed at 280 nm (protein) and 254 nm (254/280 nm ratio probes Cu-loading of Atox1 ( Niemiec *et al.* 2012, 2015); ligand-to-metal charge transfer) showed that samples that had been subjected to agitation and incubation, i.e., 'amyloid inhibitory condition' contained significant fractions of monomeric αS (cf. Fig. S2A) and Atox1, in accord with no amyloid formation.

SEC analysis of freshly mixed samples, mimicking the Biacore experiments, showed the absence of a detectable Cu-Atox1/αS complex but according to the 254/280 nm ratio of the resulting Atox1 peak, Cu had been removed from Atox1 (Fig. S3). Inductively coupled plasma mass spectrometry (ICP-MS) elemental analysis of Cu in the αS fractions (cannot be determined via 254/280 nm absorption ratio) from Cu-Atox1/αS mixtures revealed increased amounts of Cu in αS; thus, some Cu had moved from Atox1 to αS (Fig. 3*b*). Because the eluted protein fractions contain protein in concentrations near the determined dissociation constant for the Cu-Atox1/αS complex, it is reasonable that the Cu-Atox1/αS complex detected in Biacore dissociates when running through SEC. If Cu is bridging the ternary

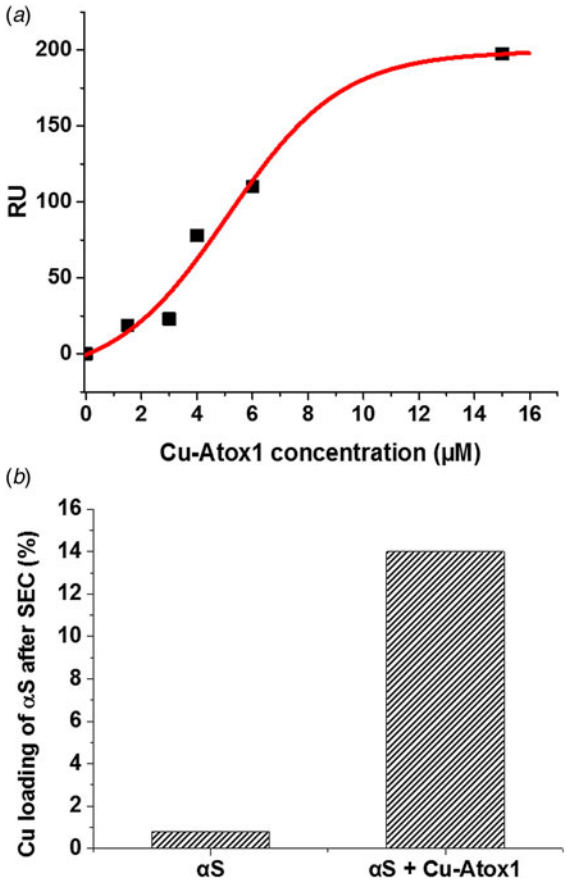


**Fig. 3.** (*a*) Binding data from Biacore experiments for the interaction of Cu-Atox1 with an αS-coated surface. (*b*) Cu content (shown as % of total protein, assuming one Cu per protein) determined by ICP-MS for the αS peak eluted on a Superdex 75 column of αS alone and the mixture αS + Cu-Atox1.

complex, it is indeed reasonable that some Cu is found in αS upon dissociation.

Our findings suggest that Cu(I)-loaded Atox1 can form a Cu(I)-dependent complex with αS monomers that results in blockage of αS amyloid formation (Fig. 4). The apo-form of Atox1 may interact weakly with αS, and this appears to delay aggregation to some extent. The Atox1–Cu–αS complex appears to involve bridging of Cu(I), as, if the complex is dissociated (eg. during SEC), some of the Cu(I) is then found in αS. Cu(I) can bind to sites in both N- and C-termini in αS (Binolfi *et al.* 2006, 2011; Camponeschi *et al.* 2013; De Ricco *et al.* 2015a), see Fig. 1*a*. In aggregation experiments with a truncated variant of αS (αS

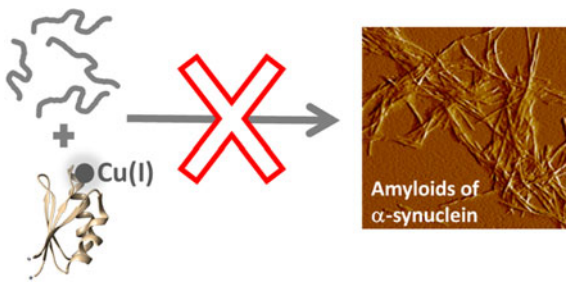


**Fig. 4.** Cartoon illustration of the main conclusion of this study, i.e., that Cu-loaded Atox1 blocks monomeric αS from aggregation into amyloid fibers *in vitro*.

residues 1–97; i.e., lacking the C-terminal 43 residues), we found Cu(I)-Atox1 to inhibit the amyloid formation of the αS variant but apo-Atox1 had no effect (Fig. S4). Because these results are similar to those found for wild-type αS, we propose that Cu(I)-Atox1 interacts with the N-terminal Cu(I) site of αS. This interaction may sterically block assembly of core regions of αS into amyloid fibers, but further mechanistic studies are desired.

In conclusion, we propose that metal-dependent chaperoning, exemplified by Cu(I)-Atox1, may be another cellular mechanism, in addition to the protein chaperone network, that controls the proteome. In similarity with respect to the outcome but opposite in terms of the role of the metal, metallothioneins can scavenge Cu(II) and Zn(II) from amyloidogenic peptides and protect against aggregation (Atrian-Blasco *et al.* 2017; Okita *et al.* 2017). For the specific case of PD, a significant decrease in total tissue Cu in substantia nigra has been reported (Davies *et al.* 2014; Okita *et al.* 2017). In addition to perturbing the antioxidant activity of Cu-dependent SOD1, our results imply that this reduction in tissue Cu may also abolish a Cu(I)-dependent chaperoning ability of Atox1; both being alterations that would further promote PD.

### Box: speculation

In addition to the myriad of well-established chaperone and chaperonin proteins that aid in protein folding and quality control, we propose that metal-dependent chaperoning, here shown for a cytoplasmic copper chaperone, is an additional cellular process that modulates and controls the proteome. We speculate that interactions between the copper chaperone Atox1 and αS normally hold back αS amyloid formation and this interaction may also deliver copper ions to αS for (yet, unknown) metal-dependent αS functions. In contrast, when cellular metal homeostasis and/or redox status is disrupted, metal-dependent chaperone interactions may be abolished and deleterious aggregation of amyloidogenic proteins (such as αS) can flourish.

**Supplementary material.** The supplementary material for this article can be found at https://doi.org/10.1017/S0033583518000045

**Acknowledgement.** We thank Stellan Holgersson (Chalmers) for ICP-MS analysis.

**Financial support.** Funding is acknowledged from the Knut and Alice Wallenberg Foundation, the Swedish Research Council, the Olle Engkvist foundation and the Chalmers Foundation.

**Conflict of interest.** None.

## References

**Atrian-Blasco E *et al.*** (2017) Chemistry of mammalian metallothioneins and their interaction with amyloidogenic peptides and proteins. *Chemical Society Reviews* **46**, 7683–7693.

**Binolfi A *et al.*** (2006) Interaction of alpha-synuclein with divalent metal ions reveals key differences: a link between structure, binding specificity and fibrillation enhancement. *Journal of the American Chemical Society* **128**, 9893–9901.

**Binolfi A *et al.*** (2011) Exploring the structural details of Cu(I) binding to alpha-synuclein by NMR spectroscopy. *Journal of the American Chemical Society* **133**, 194–196.

**Blockhuys S *et al.*** (2017) Defining the human copper proteome and analysis of its expression variation in cancers. *Metallomics* **9**, 112–123.

**Blockhuys S and Wittung-Stafshede P** (2017) Copper chaperone Atox1 plays role in breast cancer cell migration. *Biochemical and Biophysical Research Communications* **483**, 301–304.

**Boal AK and Rosenzweig AC** (2009) Structural biology of copper trafficking. *Chemical Reviews* **109**, 4760–4779.

**Brown DR** (2013) α-Synuclein as a ferrireductase. *Biochemical Society Transactions* **41**, 1513–1517.

**Camponeschi F *et al.*** (2013) Copper(I)-alpha-synuclein interaction: structural description of two independent and competing metal binding sites. *Inorganic Chemistry* **52**, 1358–1367.

**Chorell E *et al.*** (2015) Bacterial chaperones CsgE and CsgC differentially modulate human alpha-synuclein amyloid formation via transient contacts. *PLoS ONE* **10**, e0140194.

**Davies KM *et al.*** (2014) Copper pathology in vulnerable brain regions in Parkinson's disease. *Neurobiology of Aging* **35**, 858–866.

**Davies KM *et al.*** (2013) Localization of copper and copper transporters in the human brain. *Metallomics* **5**, 43–51.

**Davies KM *et al.*** (2016) Copper dyshomoeostasis in Parkinson's disease: implications for pathogenesis and indications for novel therapeutics. *Clinical Science (Lond)* **130**, 565–574.

**De Feo CJ *et al.*** (2009) Three-dimensional structure of the human copper transporter hCTR1. *Proceedings of the National Academy of Sciences of the United States of America* **106**, 4237–4242.

**De Ricco R *et al.*** (2015a) Differences in the binding of copper(I) to alpha- and beta-synuclein. *Inorganic Chemistry* **54**, 265–272.

**De Ricco R *et al.*** (2015b) Copper(I/II), alpha/beta-synuclein and amyloid-beta: menage a Trois? *Chembiochem* **16**, 2319–2328.

**Fink AL** (2006) The aggregation and fibrillation of alpha-synuclein. *Accounts of Chemical Research* **39**, 628–634.

**Galvin JE *et al.*** (1999) Pathobiology of the Lewy body. *Advances in Neurology* **80**, 313–324.

**Hatori Y and Lutsenko S** (2013) An expanding range of functions for the copper chaperone/antioxidant protein Atox1. *Antioxidants & Redox Signaling* **19**, 945–957.

**Horcas I *et al.*** (2007) WSXM: a software for scanning probe microscopy and a tool for nanotechnology. *Review of Scientific Instruments* **78**, 013705.

**Horvath I *et al.*** (2012) Mechanisms of protein oligomerization: inhibitor of functional amyloids templates alpha-synuclein fibrillation. *Journal of the American Chemical Society* **134**, 3439–3444.

**Horvath I and Wittung-Stafshede P** (2016) Cross-talk between amyloidogenic proteins in type-2 diabetes and Parkinson's disease. *Proceedings of the National Academy of Sciences of the USA* **113**, 12473–12477.

**Lutsenko S, LeShane ES and Shinde U** (2007) Biochemical basis of regulation of human copper-transporting ATPases. *Archives of Biochemistry and Biophysics* **463**, 134–148.

**Montes S *et al.*** (2014) Copper and copper proteins in Parkinson's disease. *Oxidative Medicine and Cellular Longevity* **2014**, 147251.

**Niemiec MS, Dingeldein AP and Wittung-Stafshede P** (2015) Enthalpy-entropy compensation at play in human copper ion transfer. *Scientific Reports* **5**, 10518.

**Niemiec MS, Weise CF and Wittung-Stafshede P** (2012) In vitro thermodynamic dissection of human copper transfer from chaperone to target protein. *PLoS ONE* **7**, e36102.

**Ohrvik H and Thiele DJ** (2014) How copper traverses cellular membranes through the mammalian copper transporter 1, Ctr1. *Annals of the New York Academy of Sciences* **1314**, 32–41.

**Okita Y *et al.*** (2017) Metallothionein, copper and alpha-synuclein in alpha-synucleinopathies. *Frontiers in Neuroscience* **11**, 114.

**Tottey S, Harvie DR and Robinson NJ** (2005) Understanding how cells allocate metals using metal sensors and metallochaperones. *Accounts of Chemical Research* **38**, 775–783.

**Waldron KJ *et al.*** (2009) Metalloproteins and metal sensing. *Nature* **460**, 823–830.

**Winner B *et al.*** (2011) In vivo demonstration that alpha-synuclein oligomers are toxic. *Proceedings of the National Academy of Sciences of the United States of America* **108**, 4194–4199.